Proceedings of the ASME 2019
International Design Engineering Technical Conferences
and Computers and Information in Engineering Conference
IDETC/CIE2019
August 18-21, 2019, Anaheim, CA, USA

DETC2019-97826

COMPUTATIONAL FLUID DYNAMICS SIMULATION OF FLOW OF EXHALED PARTICLES FROM POWERED-AIR PURIFYING RESPIRATORS

Susan S. Xu
National Institute for Occupational Safety and Health, Centers for Disease Control and Prevention, Pittsburgh, Pennsylvania

Zhipeng Lei*
National Institute for Occupational Safety and Health, Centers for Disease Control and Prevention
Pittsburgh, Pennsylvania
wrt8@cdc.gov

Ziqing Zhuang
National Institute for Occupational Safety and Health, Centers for Disease Control and Prevention, Pittsburgh, Pennsylvania

Michael Bergman
National Institute for Occupational Safety and Health, Centers for Disease Control and Prevention, Pittsburgh, Pennsylvania

ABSTRACT

In surgical settings, infectious particulate wound contamination is a recognized cause of post-operative infections. Powered air-purifying respirators (PAPRs) are widely used by healthcare workers personal protection against infectious aerosols. Healthcare infection preventionists have expressed concern about the possibility that infectious particles expelled from PAPR exhalation channels could lead to healthcare associated infections, especially in operative settings where sterile procedural technique is emphasized.

This study used computational fluid dynamics (CFD) modeling to simulate and visualize the distribution of particles exhaled by the PAPR wearer. In CFD simulations, the outward release of the exhaled particles, i.e., ratio of exhaled particle concentration outside the PAPR to that of inside the PAPR, was determined. This study also evaluated the effect of particle sizes, supplied air flow rates, and breathing work rates on outward leakage.

This simulation study for the headform and loose-fitting PAPR system included the following four main steps: (1) preprocessing (establishing a geometrical model of a headform wearing a loose-fitting PAPR by capturing a 3D image), (2) defining a mathematical model for the headform and PAPR system, and (3) running a total 24 simulations with four particle sizes, three breathing workloads and two supplied-air flow rates (4x3x2=24) applied on the digital model of the headform and PAPR system, and (4) post-processing the simulation results to visually display the distribution of exhaled particles inside the PAPR and determine the particle concentration of outside the PAPR compared with the concentration inside. We assume that there was no ambient particle, and only exhaled particles existed. The results showed that the ratio of the exhaled particle concentration outside to inside the PAPR were influenced by exhaled particle sizes, breathing workloads, and supplied-air flow rates. We found that outward concentration leakage from PAPR wearers was approximately 9% with a particle size of 0.1 and 1 μm at the light breathing and 205 L/min supplied-air flow rates, which is similar to the respiratory physiology of a health care worker in operative settings, The range of the ratio of exhaled particle concentration leaking outside the PAPR to the exhaled particle concentration inside the PAPR is from 7.6% to 49. We found that supplied air flow rates and work rates have significant impact on outward leakage, the outward concentration leakage increased as particle size decreased, breathing workload increased, and supplied-air flow rate decreased. The results of our simulation study should help provide a foundation for future clinical studies.

KEYWORDS

Exhaled particles, outward leakage, powered air-purifying respirators, Computational Fluid Dynamics Simulation, Surgical setting

INTRODUCTION

Contamination of surgical fields is a widely recognized cause of post-operative infections, and the dispersion of pathogens through the air is known as a cause of healthcare-associated (HAIs) infections [1, 2]. Approximately 722,000 HAIs were identified U.S. acute care hospitals in 2001, including an estimated 157,500 surgical site infections (SSIs), from

inpatient surgery [3]. The use respiratory protection and other personal protective equipment (PPE) by healthcare personal (HCP) is an important measure to reduce the chances aerosol transmission.

Protection of HCP from airborne bacteria may be improved by incorporating the use of plastic face shields, which afford a higher level of protection from contamination [4]. Recently, powered air-purifying respirators (PAPRs) have been increasingly used by HCP [5] for self-protection. PAPRs used in healthcare typically use a battery operated blower and one or more high-efficiency particulate air (HEPA) filter(s) to provide the wearer with purified air. PAPRs can be separated into two classes depending on how they're worn: a tight-fitting class that forms a seal with the wearer's skin and a loose-fitting class comprised of hoods or helmets that reduce the wearer's exposure to ambient aerosols by ensuring constant air-flow from the filter to the loose opening of the respirator at the neck or shoulders.

The current study addresses the flow of particles out of loose-fitting PAPRs. PAPR hood designs can fully cover the wearer's head and neck to prevent skin contact with body fluids from an infected person. Hence, loose-fittings PAPRs are well suited for use by healthcare workers during aerosol generating procedures that sometimes pose a higher risk of exposure than routine healthcare duties. There is debate about where the exhaled particles released from PAPR facepiece, therefore, further investigation of the factors determining particle trajectory from PAPRs is needed. This lack of information has inhibited the use of PAPRs. There are situations that healthcare workers and safety professionals would potentially choose a PAPR, but concerns about exhaled/expelled potentially infectious particulates may contaminate the surgical site. This topic has been the source of controversy among healthcare professionals working in the operating room (OR) [6].

There are four respiratory actions that produce airborne particles or droplets: mouth breathing, nose breathing, coughing/sneezing, and talking. In general, coughing produces the largest droplet concentrations and nose breathing the least. Papineni and Rosenthal [7] found the preponderance of particles is less than 1 μm in size during normal breathing and talking. Droplet transmission is pertinent to larger particles that are expelled and rapidly settle to a surface (e.g., interior surface of PAPR hood), usually within one minute of production, and droplet transmission therefore relies on relatively close proximity to the source [8]. The exhaled particles from PAPR wearers are of sufficient size as to be significantly affected by gravity, hence falling, rather than remaining atomized and being expelled from the OR by the air exchange system. Yan, Grantham [9] assessed infectious virus in exhalation of symptomatic seasonal influenza cases. The results showed that viral RNA of fine and coarse aerosols were positively associated with body mass index and number of coughs, suggesting that transmission of infectious virus in exhalation may related to breathing patterns.

The authors are aware of only two pilot experimental studies to compare the particle concentration in an OR with and without PAPRs being used due to the expense, time and specialized facilities required. Kim and Hale [10] conducted a pilot study to examine the use of a PAPR in the OR and found no discernable differences in the particulate counts at the surgical table when the PAPR-hood system was turned on or off (ranges: 1700-1850 particles/cm3). Their conclusion was that the hooded PAPR did not increase particulate transfer to the surgical field. Grinshpun [11] conducted another pilot study to simulate PAPR wearers in an OR to assess the bacterial contamination of sterile field surfaces. He found that when comparing the respiratory and control groups per each agar plate location separately, there was no statistically significant difference in the mean contamination values associated with a specific agar plate location for either of the PAPR or N95 respirators tested. On average, the bacterial contamination of sterile fields by a pair of subjects operating in an OR-simulating facility while wearing either PAPRs or N95 respirators is significantly higher than that obtained in both negative control tests.

Because of the limited empiric particulate data on the use of PAPR in an OR, computational fluid dynamics (CFD), a numerical method for simulating fluid and temperature flow, can be appropriate in this research topic. Our previous study constructed digital headform models with the biomechanics of breathing to simulate the protection of loose-fitting PAPRs against particles using CFD [12]. The CFD PAPR model was based on a loose-fitting PAPR system that had a loose-fitting facepiece. In the CFD simulations, the PAPR supplied-air and the cyclic breathing air vented inside the PAPR. The challenge particles, which were the particles outside of the PAPR breathing zone, were introduced at the loose-fitting area where the PAPR loosely fits the headform. The particle concentration of inhalation air was simulated using Eulerian-Lagrangian particle tracking, in which particles are allowed to move relative to the air flow. In a later study from our group, the computational results of the CFD PAPR models were validated using actual experimental data [13].

This study focused on three objectives: (1) Utilize CFD modeling to simulate and visualize the distribution of particles exhaled by the PAPR wearers in the breathing zone; (2) Determine the outward leakage of the exhaled particles, i.e., ratio of exhaled particle concentration outside the PAPR to that inside the PAPR as a function of exhaled particle concentrations and sizes; (3) Evaluate the effect of supplied-air flow rates and work rates on outward leakage to better understand the relationships among flow rate, work rate, and outward leakage.

METHODS

PAPR Model

The MaxAir® Systems 78SP-36 cuff system with disposable cuff (Bio-Medical Devices, Inc., Irvine, CA) pictured in Figure 1, a popular loose-fitting PAPR model used in healthcare worker settings, was selected for this study. It was a helmet-style where both the filter and blower motor are contained in the helmet. A digital loose-fitting PAPR was created by scanning the geometries of the components of the MaxAir®

model and using additional surface processing to achieve a model suited for CFD.

Figure 1. MaxAir® 78SP-36 cuff system (Photos Credit: NIOSH/NPPTL)

The digital PAPR model had supplied-air venting holes that were the same number (10) and size (10 mm diameter) as in the PAPR prototype. This study chose two supplied-air flow rates 100 and 205 L/min. 170 L/min is the minimum current NIOSH certification required air flow rates for loose-fitting PAPRs. A higher supplied-air flow rate of 205 L/min was evaluated in this study because flow rates for PAPRs tend to exceed the NIOSH minimum flow rate.

Head model

In the CFD model, the NIOSH medium-size digital headform, representing approximately 50% of the current U.S. workforce [14], was used to simulate the wearer of a loose-fitting PAPR. The headform used a cylindrical tube, 2 cm in diameter and 10 cm long, connected to the headform's mouth as a breathing airway through which breathing air passes through the mouth and in and out of the airway during CFD simulations.

Three respiratory minute ventilations VE (L/min) and breathing rates f (breaths/minute) were selected in this study, as listed in Table 1. They were at Light 25 L/min with f=20, Moderate 48 L/min with f=27 and Heavy 88 L/min with f=32. This three work rate were chosen to provide a range of respiration from light work to heavy exertion to simulate health care workers in hospitals.

Table 1: the task activities with the work rate and minute ventilation

Task activity	Work rate	Minute ventilation (L/min)
Light work (standing or working in an operating room and carrying weight < 25 lbs)	Light	25
Moderate exertion (lifting or moving patients i.e., weight > 100 lbs)	Moderate	48
Heavy work (Emergency situation)	Heavy	88

CFD Model of PAPR-headform

We constructed a CFD model of the PAPR-headform to mimic the situation in which a loose-fitting PAPR is donned on a manikin. The digital headform virtually donned the digital PAPR model, generating a volume between the headform and the loose-fitting PAPR which we refer to as the breathing zone into which both the breathing air and the supplied-air streamed. The breathing zone was divided into 913,653 hexahedral cells using the tool SnappyHexMesh provided by OpenFOAM software (version 4.0, the OpenFOAM Foundation Ltd, London, United Kingdom).

The surface of the CFD model was split into different boundaries, including the surface wall, supplied-air venting, breathing venting, and loose-fitting area, presented in Figure 2. The surface wall consisted of PAPR and headform surfaces and was applied the non-slip boundary condition, i.e., the flow velocity at the boundary is held at zero. A velocity inlet boundary condition was modeled using a constant flow through the supplied-air venting into the PAPR breathing zone. The breathing venting was also applied the velocity inlet boundary condition but had sinusoidal flow rate to simulate the cyclic breathing pattern, including both inhalation and exhalation. The area where the PAPR loosely fits the headform at the neck had an approximately 10 mm gap about 80 mm wide and 15 mm long. The pressure outlet boundary condition was defined at the loose-fitting area to simulate the air flow exiting the PAPR to the atmosphere at zero gauge pressure.

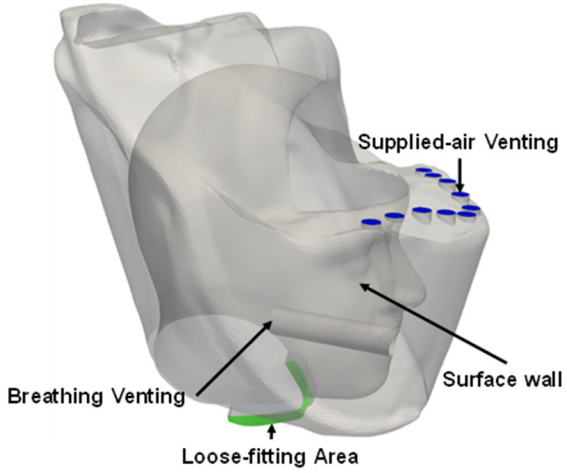

Figure 2. CFD model of PAPR-headform

CFD simulation

This simulation study will innovatively develop a CFD model to run 24 simulations with four particle sizes, three workloads, and two supplied air flow rates (4x3x2=24) applied on a loose-fitting PAPR donned on a digital headform.

In the CFD solver, we defined the mass continuity and the Navier-Stokes equations to describe the interaction of the breathing air flow and supplied-air flow in the PAPR breathing

zone, using the assumption of unsteady incompressible flow. The Eulerian-Lagrangian particle tracking technique was used to track particles in the velocity fields of the CFD model. We assumed that only air drag force influences the particle movement and the particle diffusion can be neglected so that the governing equations for the movement of a spherical particle are as follows:

$$m_p \frac{d\boldsymbol{U_p}}{dt} = \boldsymbol{F_D} \quad (1)$$

$$\frac{\mathrm{d}\mathbf{X_P}}{\mathrm{dt}} = \boldsymbol{U_p} \quad (2)$$

where m_p is the particle mass, $\boldsymbol{U_p}$ is the particle velocity, $\boldsymbol{F_D}$ is the drag force per unit particle mass, and X_p is the particle position [18]. $\boldsymbol{F_D}$ is dependent on the particle Reynolds number:

$$\boldsymbol{F_D} = \frac{24\nu}{d}\frac{3\rho}{4d\rho_P}(1 + 0.15Re_P^{0.687})(\boldsymbol{U} - \boldsymbol{U_p}) \quad (3)$$

where ν is the kinematic viscosity, d is the particle aerodynamic diameter, ρ is the air density, ρ_p is the particle density, $\boldsymbol{U}$ is the air velocity, and Re_p is the particle Reynolds number. Re_p is defined as:

$$Re_p = \frac{d|\boldsymbol{U}-\boldsymbol{U_p}|}{\nu}. \quad (4)$$

We assumed that when particles touched the surface wall boundary, they deposited on the boundary and did not rebound back to the air.

The pisoFoam solver (in OpenFOAM) with the PISO (Pressure Implicit with Splitting of Operators) algorithm was used to perform the CFD simulation since the solver assumes that the flow is transient and incompressible and has a turbulent effect. Each simulation calculated for the duration of three breathing cycles with 0.001-second time-steps; at each time-step, the pressure field and the velocity field inside the PAPR breathing zone were determined. When the breathing was in the exhalation phase, particles with a uniform size and concentration of 100 particles/cm^3, were generated in the exhaled air at the breathing airway. Note that this is a nominal concentration for demonstration purposes and not a realistic concentration. Based on Equations (1-4), particle movements were tracked to calculate the number of particles leaking out of the PAPR through the loose-fitting faceseal.

Since the flow rate and the particle concentration of the exhaled air from the mouth opening were known, we can compute the total number of exhaled particles from the mouth. After the CFD simulations, we monitored the number of exhaled particles leaking outside the PAPR. Then, in each CFD simulation we determined the outward particle leakage, i.e., the ratio of exhaled particle number leaking outside the PAPR to the inside the PAPR which are exhaled particle number from the mouth:

$$Outward\ Particle\ Leakage = \frac{exhaled\ particle\ number\ outside\ the\ PAPR}{exhaled\ particle\ number\ inside\ the\ PAPR} \quad (5)$$

After the CFD simulations, we also monitored the volume of the air venting outside the PAPR, so that the exhaled particle concentration leaking outside the PAPR can be estimated. In each CFD simulation we determined the outward concentration leakage, i.e., the ratio of exhaled particle concentration leaking outside the PAPR to the exhaled particle concentration inside the PAPR:

$$Outward\ Concentration\ Leakage = \frac{exhaled\ particle\ concentration\ outside\ the\ PAPR}{exhaled\ particle\ concentration\ inside\ the\ PAPR} \quad (6)$$

RESULTS

The particle distribution of a CFD simulation (heavy breathing, supplied-air flow rate 205 L/min, and particle size 1 μm) at different time instances is showed in Figure 3. During the first breathing cycle's exhalation, displayed in the first three time instances, the exhaled particles moved out of the mouth opening and occupied the region close to the frontal face, and part of the exhaled particles leaked outside of the PAPR through the loose-fitting faceseal. During the first breathing cycle's inhalation, presented in the fourth and fifth time instances, part of the exhaled particles were inhaled into the mouth opening. After the first breathing cycle, shown in the sixth time instance, part of the exhaled particles occupied most of the region inside the PAPR, part of them deposited on the face or PAPR, part of them were inhaled, and the rest leaked out of the PAPR.

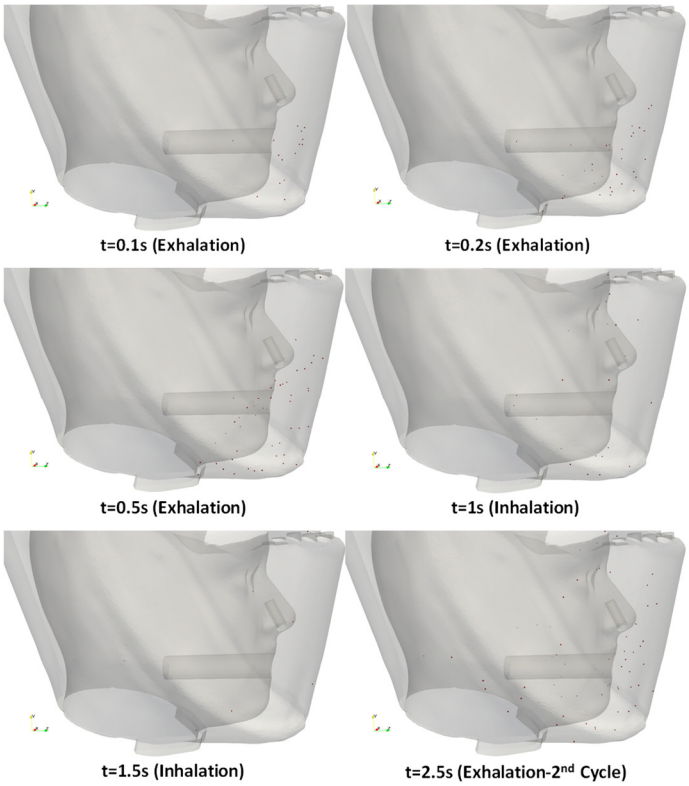

Figure 3: Particle distribution inside the PAPR inlet covering at different time instances of a breathing cycle (heavy workload, supplied-air flow rate 205 L/min, and particle size 1 μm).

Figure 4 presents outward particle leakage at different particle sizes, breathing conditions, and supplied-air flow rates cumulated over all three breaths. The particle outward leakage indicates the percentage of exhaled particles leaking outside of the PAPR. The highest particle outward leakage, 75.50%, appeared in the CFD simulation of particle size 0.1 µm, light breathing, and supplied-air flow rate 205 L/min, and the lowest one, 32.39%, appeared in the CFD simulation of particle size 10 µm, heavy breathing, and supplied-air flow rate 100 L/min. The outward particle leakage increased as particle size decreased, breathing workload decreased, and supplied-air flow rate increased.

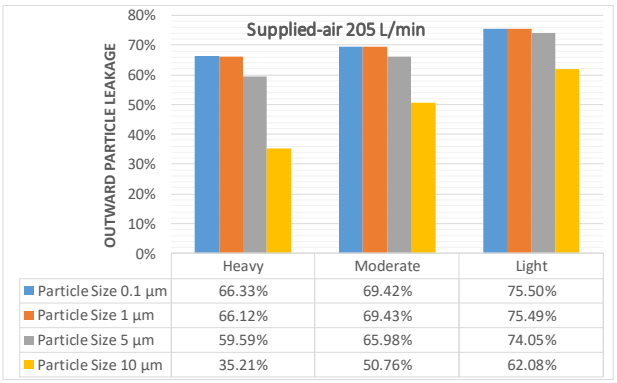

	Heavy	Moderate	Light
Particle Size 0.1 µm	66.33%	69.42%	75.50%
Particle Size 1 µm	66.12%	69.43%	75.49%
Particle Size 5 µm	59.59%	65.98%	74.05%
Particle Size 10 µm	35.21%	50.76%	62.08%

(a)

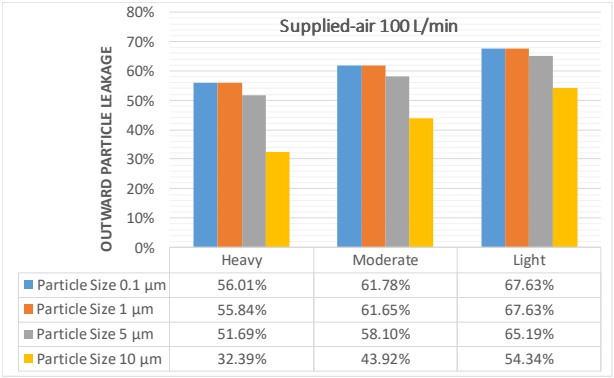

	Heavy	Moderate	Light
Particle Size 0.1 µm	56.01%	61.78%	67.63%
Particle Size 1 µm	55.84%	61.65%	67.63%
Particle Size 5 µm	51.69%	58.10%	65.19%
Particle Size 10 µm	32.39%	43.92%	54.34%

(b)

Figure 4: Particle outward leakage of different particle sizes, breathing conditions, and supplied-air flow rates; (a) supplied-air flow rate 205 L/min, and (b) supplied-air flowrate 100 L/min.

Figure 5 presents the outward concentration leakage at different particle sizes, breathing conditions, and supplied-air flow rates. The outward concentration leakage indicates the comparison between the exhaled particle concentration leaking outside the PAPR and the exhaled particle concentration inside the PAPR. The highest outward leakage concentration, 49.29%, appeared in the CFD simulation of particle size 0.1µm, heavy breathing, and supplied-air flow rate 100 L/min, and the lowest one, 7.57%, appeared in the CFD simulation of particle size 10 µm, light breathing, and supplied-air flow rate 205 L/min. The outward concentration leakage increased as particle size decreased, breathing workload increased, and supplied-air flow rate decreased.

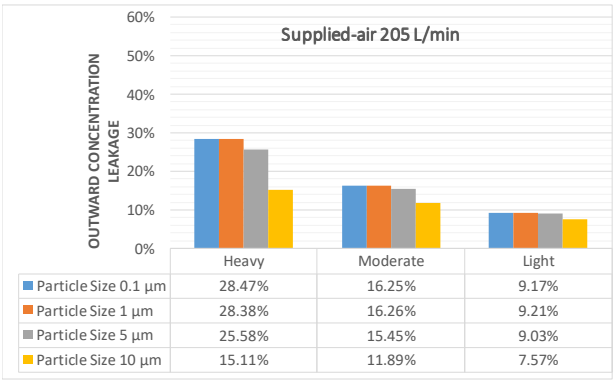

	Heavy	Moderate	Light
Particle Size 0.1 µm	28.47%	16.25%	9.17%
Particle Size 1 µm	28.38%	16.26%	9.21%
Particle Size 5 µm	25.58%	15.45%	9.03%
Particle Size 10 µm	15.11%	11.89%	7.57%

(a)

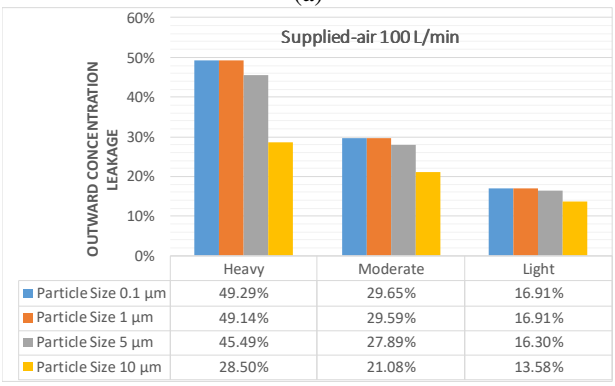

	Heavy	Moderate	Light
Particle Size 0.1 µm	49.29%	29.65%	16.91%
Particle Size 1 µm	49.14%	29.59%	16.91%
Particle Size 5 µm	45.49%	27.89%	16.30%
Particle Size 10 µm	28.50%	21.08%	13.58%

(b)

Figure 5: Concentration outward leakage of different particle sizes, breathing conditions, and supplied-air flow rates; (a) supplied-air flow rate 205 L/min, and (b) supplied-air flowrate 100 L/min.

DISCUSSIONS

To analyze the outward leakage of exhaled particles from PAPR wearers, we defined two parameters, the particle outward leakage and the concentration outward leakage (see Equation 5 and 6). The particle outward leakage evaluated the number of exhaled particles leaking outside of the PAPR, while the outward concentration leakage evaluated the concentration of exhaled particle leaking outside of the PAPR. The latter is more related to the experimental measurement in Kim and Hale [10], which measured the exhaled particle concentration outside PAPR. Because the PAPR system used in the CFD simulations has a loose-fitting face cover hood, unlike the hood style in the PAPR system used in Kim and Hale [10], exhaled particles were able to move outside of the PAPR through the gap at the loose-fitting faceseal.

The CFD simulation results show that the particle size, breathing conditions, and the supplied-air flow rates all have an impact on the outward leakage. Coarse particles (size $\geq$ 5 µm) are more likely to deposit inside PAPR than fine particles (size $<$ 5 µm). Hence, the increase of particle size would decrease both

the outward particle leakage and the concentration outward leakage. Since the supplied-air makes it easier for the particles to leak outside of PAPR but dilutes the particle concentration, the increase of supplied-air flow rate would increase the particle outward leakage but decrease the outward concentration leakage. Although the heavy breathing air flow makes the particle more likely to deposit inside PAPR, it produces more exhaled particles, reducing the dilution level from the supplied-air flow. As a consequence, the increase of the breathing workload would decrease the outward particle leakage but increase the outward concentration leakage.

Limitations in this numerical study included that we ignored the particle dispersion that is the random motions of particles due to diffusion or turbulence, and that only mouth breathing was considered in this study. Additionally, empiric particulate data is needed to validate the CFD results.

Future studies will include more PAPR systems into the CFD simulations, especially the PAPR systems with double-shrouded hoods that extend to the surgical gown. Compare CFD simulation of flow of exhaled particles from surgical N95 Respirators and PAPRs. Using the CFD model of PAPR-headform, we can optimize the design of PAPR systems to reduce the contamination of exhaled particles in surgical settings.

CONCLUSIONS

The CFD simulation results visually show the distribution of exhaled particles by the PAPR wearers in the breathing zone. The outward leakage of the exhaled particles, i.e., ratio of exhaled particle concentration outside the PAPR to that inside the PAPR, was determined as a function of exhaled particle concentrations and sizes. We found that outward concentration leakage from PAPRs is about 9% for a particle size of 0.1 and 1 μm at light breathing and 205 L/min supplied-air flow rate which is similar to a healthcare worker's breathing workload in an OR. The range of the ratio of exhaled particle concentration leaking outside the PAPR to the exhaled particle concentration inside the PAPR is from 7.6% to 49%. Supplied air flow rates and work rates have significant impact on outward leakage, the outward concentration leakage increased as particle size decreased, breathing workload increased, and supplied-air flow rate decreased.

The significance of this study is for providing foundation for future laboratory and clinical research related to respirator effectiveness in surgical or procedural settings. Also, the simulation results should inform future studies about protective equipment selection in surgical settings. CFD modeling can help manufacturers to evaluate respirator leakage performance for product development. Furthermore, this study will provide the groundwork for development of future clinical studies.

DISCLAIMER

The findings and conclusions in this study are those of the author(s) and do not necessarily represent the official position of the National Institute for Occupational Safety and Health, Centers for Disease Control and Prevention. Mention of a company or product name does not constitute endorsement by NIOSH.

ACKNOWLEDGMENTS

The authors thank the following persons for their contributions: Ronald Shaffer, Harold Boyles, Debbie Novak, and Bill King.

REFERENCES

1. Da Zhou, C., P. Sivathondan, and A. Handa, *Unmasking the surgeons: the evidence base behind the use of facemasks in surgery.* Journal of the Royal Society of Medicine, 2015. **108**(6): p. 223-228.
2. Lipp, A. and P. Edwards, *Disposable surgical face masks for preventing surgical wound infection in clean surgery.* Cochrane Database of Systematic Reviews, 2014(2).
3. CDC. *Healthcare-associated Infections Data*. 2018 Feb 4, 2019]; Available from: https://www.cdc.gov/hai/data/index.html.
4. Skinner, M. and B. Sutton, *Do Anaesthetists Need to Wear Surgical Masks in the Operating Theatre? A Literature Review with Evidence-Based Recommendations.* Anaesthesia and intensive care, 2001. **29**(4): p. 331-338.
5. Wizner, K., et al., *Prevalence of Respiratory Protective Devices in U.S. Health Care Facilities:Implications for Emergency Preparedness.* Workplace Health & Safety, 2016. **64**(8): p. 359-368.
6. Sreeramoju, P.V. and J. Cadena, *Airborne Precautions and Personal Protective Equipment: The Powered Air-Purifying Respirator-Only Approach*, in *Infection Prevention*. 2018, Springer. p. 285-291.
7. Papineni, R.S. and F.S. Rosenthal, *The Size Distribution of Droplets in the Exhaled Breath of Healthy Human Subjects.* Journal of Aerosol Medicine, 1997. **10**(2): p. 105-116.
8. Wurie, F., et al., *Characteristics of exhaled particle production in healthy volunteers: possible implications for infectious disease transmission.* F1000Research, 2013. **2**: p. 14-14.
9. Yan, J., et al., *Infectious virus in exhaled breath of symptomatic seasonal influenza cases from a college community.* 2018. **115**(5): p. 1081-1086.
10. Kim, Y. and M. Hale, *Pilot Study to Examine the Use of a Powered Air Purifying Respirator (PAPR) in the Operating Room.* American Journal of Infection Control, 2017. **45**(6): p. S84.
11. Grinshpun, S., *Simulation Study: Does the Air Exhaled from a PAPR Wearer Contaminate the Sterile Field in an Operating Room? Final Report*. 2016.
12. Lei, Z., Z. Zhuang, and M. Bergman. *Application of digital human modeling for evaluating loose-fitting powered air-purifying respirators*. in *Proceedings of the 5th international digital human modeling symposium*. 2017.
13. Bergman, M., et al. *Validation of Computational Fluid Dynamics Models for Evaluating Loose-Fitting Powered Air-Purifying Respirators*. in *Congress of the International Ergonomics Association*. 2018. Springer.

14. Benson, S. and D. Viscusi, *Digital 3-D headforms with facial features representative of the current US workforce AU - Zhuang, Ziqing.* Ergonomics, 2010. **53**(5): p. 661-671.
15. 15. Adams, W.C., *Measurement of breathing rate and volume in routinely performed daily activities: final report, contract no. A033-205*. 1993: The Division.
16. Anderson, N.J., et al., *Peak inspiratory flows of adults exercising at light, moderate and heavy work loads.* Journal-international society for respiratory protection, 2006. **23**(1/2): p. 53.
17. Lindsley, W.G., et al., *Dispersion and exposure to a cough-generated aerosol in a simulated medical examination room.* Journal of occupational and environmental hygiene, 2012. **9**(12): p. 681-690.
18. Tsuda, A., F.S. Henry, and J.P. Butler, *Particle transport and deposition: basic physics of particle kinetics.* Comprehensive Physiology, 2013. **3**(4): p. 1437-1471.